Electronic Supplementary Material (ESI) for Nanoscale.
This journal is © The Royal Society of Chemistry 2017

Electronic Supplementary Information

The thermodynamic influence of solution-phase additives in shape-controlled nanocrystal synthesis

Xin Qi and Kristen A. Fichthorn*‡

Dept. of Chemical Engineering, The Pennsylvania State University, University Park, Pennsylvania 16802, United States. E-mail: fichthorn@psu.edu; Fax: +01 814 865 7846; Tel: +01 814 863 4807

‡ Also in the Dept. of Physics

1 Molecular Dynamics Simulations

1.1 Simulated Systems

The dimensions and number of particles for all simulated systems are given in Table S1.

Table S1: Additional information on MD systems

		Number of atoms		Lx (Å)		Ly (Å)		Lz (Å)	
		Ag(100)	Ag(111)	Ag(100)	Ag(111)	Ag(100)	Ag(111)	Ag(100)	Ag(111)
Half PVP monolayer coverage	Step 1	68427	66483	52.50	52.50	52.50	50.52	105.23	107.94
	Step 2	68427	66483	52.50	52.50	52.50	50.52	105.23	107.94
	Step 3	37323		52.50	52.50	52.50	50.52	105.23 to 55.74	
	Step 4	37323		52.50	52.50	52.50	50.52	55.74	
Full PVP monolayer coverage	Step 1	69462	67518	52.50	52.50	52.50	50.52	108.65	111.48
	Step 2	69462	67518	52.50	52.50	52.50	50.52	108.65	111.48
	Step 3	38358		52.50	52.50	52.50	50.52	108.65 to 59.15	
	Step 4	38358		52.50	52.50	52.50	50.52	59.15	
LJ particle study	Step 1	68427	66483	52.50	52.50	52.50	50.52	102.88	105.48
	Step 2	68427	66483	52.50	52.50	52.50	50.52	102.88	105.48
	Step 3	37323		52.50	52.50	52.50	50.52	102.88 to 47.48	
	Step 4	37323		52.50	52.50	52.50	50.52	47.48	

1.2 Force fields

In simulating PVP-covered Ag surfaces in ethylene glycol (EG) solution, we use a many-body embedded-atom method (EAM) potential for Ag[1], the CHARMM force field[2] for the liquid-phase, and the Metal-Organic Many-Body (MOMB) force field to accurately reproduce all interfacial interactions identified in DFT studies.[3,4] The MOMB force field consists of three potential models, namely the Morse potential for short-range repulsion and direct bonding, the van der Waals (vdW) dispersion implemented in Grimme's DFT-D2 method[5], and an EAM-like one-way electron density supply from the solution-phase O atom to Ag with a many-body effect. All simulations are performed using a locally modified LAMMPS package[6] that adds the function for Grimme's vdW potential[5] to the original source code.

1.3 Thermodynamic Integration

The following procedures follow the description in ref. 7. Since we adopt their value for free-energy change ΔF in Step 5 and 6, we show here the simulation details in Steps 1 through 4 for half-coverage and full-coverage PVP-EG-Ag(100) and PVP-EG-Ag(111) from MD simulations.

To initiate the multi-scheme thermodynamic integration (TI) method, we insert two superimposed repulsive walls made of fictitious atoms at each solid-liquid interface [Fig. 2(b)] in the main text. The choice of walls and the interaction between the walls and atomic species in the system are given in ref. 7. In Step 1, we gradually switch on the interaction between the repulsive walls and the system, and obtain the free-energy change ΔF_1 via TI Eq. 2 in the main text. At each λ point along the TI process, the system is equilibrated before data sampling in production runs. Care must be taken to assure that each step is reversible and free of hysteresis, which occurs when the system is well equilibrated and production sampling is sufficient at each λ point.[7] We show later in this Supporting Information that our results are hysteresis free by including reverse TI paths at various places where hysteresis is likely to occur.

In Step 2 [Fig. 2(c)], we slowly turn off the solid-liquid interactions and calculate ΔF_2 using Eq. 2. Since the PVP-EG-Ag(100) and the PVP-EG-Ag(111) systems have the same liquid volume and density, they can share the same ΔF_3 and ΔF_4 for Steps 3 and 4 [Fig. 2(e) and (f)]. In Step 3, the liquid slab is converted to a bulk liquid with walls, and in Step 4 the repulsive walls are removed. We use values of ΔF_5 and ΔF_6 for the Ag(100) and Ag(111) slabs that we obtained in a previous study[7] because we use the same conditions in this study. Finally, γ_{sl} is obtained from the negative per-area total free-energy change in this process.

The number of λ points and equilibration and production time for the PVP-EG-Ag systems at each λ in TI Step 1 through 4 are given in Table S2.

Table S2: TI details for PVP-EG-Ag systems

		Number of λ points	Equilibration (ns)	Production (ns)
Half PVP monolayer coverage	**Step 1**	11	5	8
	Step 2	27	10	10
	Step 3	25	5	5
	Step 4	19	5	5
Full PVP monolayer coverage	**Step 1**	11	5	8
	Step 2	29	15	15
	Step 3	25	5	5
	Step 4	19	5	5

1.4 Generic SDA models

In our phenomenological study, we represent generic SDAs with 120 Lennard-Jones (LJ) particles and we retain the EG solvent and the Ag slabs. The interactions between the the Lennard-Jones (LJ) particle and EG and Ag are described with the CHARMM force field, and the parameters are given in Table S3.

Table S3: CHARMM force field parameters for solution phase interactions involving LJ particle

	Inner		Outer	
	epsilon (eV)	sigma (Å)	epsilon (eV)	sigma (Å)
HCA2	0.003558	2.943804	0.003558	2.943804
HCP1	0.004071	1.950007	0.004071	1.950007
CC32A	0.004499	3.442708	0.004499	3.442708
OC311	0.008330	3.322436	0.008330	3.322436
LJ	0.004000	3.500000	0.004000	3.500000

The interaction between the LJ particle and Ag is described by Eq. 3 in the main text. The values of ϵ and the corresponding zero-K binding energy on Ag(100) and Ag(111) are summarized in Table S4.

Table S4: Variations of the LJ-Ag interaction and the corresponding binding energies

ϵ (eV)	Ag(100) hollow (eV)	Ag(111) fcc (eV)
0.10	0.798	0.789
0.080	0.639	0.628
0.064	0.510	0.501
0.048	0.382	0.375
0.032	0.254	0.249
0.016	0.127	0.124
0.0	0.0	0.0

Re-equilibration with LJ particles proceeds in a similar manner as described above for PVP, except for the equilibration and production times. Due to the mobile nature of the LJ particles, the system is equilibrated for 2 ns in the NPT ensemble and 3 ns in the NVT ensemble prior to the TI steps. Both the equilibration and production time at each λ point is 3 ns. Step 2 for the LJ-EG-Ag systems is divided into Step 2-1 and Step 2-2. In Step 2-1 the interaction between

the LJ particles and Ag is turned off and the EG-Ag interaction is turned off in Step 2-2. In this way, we avoid repetitive computing of the EG-Ag interaction for every LJ-Ag interaction set.

The number of λ points at each λ for systems with LJ particles are given in Table S5. Step 2 is divided into two stages, with the LJ-Ag interactions turned off in Step 2-1 and EG-Ag interactions turned off in Step 2-2.

Table S5: TI details for LJ systems

	Interaction strength	Number of λ points
Step 1	All	11
Step 2-1	0.10	28
	0.08	27
	0.064	25
	0.048	21
	0.032	17
	0.016	11
Step 2-2	All	20
Step 3	All	12
Step 4	All	12

Using the multi-scheme TI method, we calculate ΔF in Step 1 through 4 for systems with the LJ-Ag interactions given in Table S4. These values are added to ΔF in Step 5 and 6 in the same way as PVP to obtain γ_{sl}.

2 Supporting Results

2.1 Free-energy Change

All free-energy changes are summarized in Table S6. The free-energy changes in Steps 5 and 6 are taken from our previous study, where we employed identical Ag slabs to those in this study[7].

Table S6: Free-energy change in each step for all systems.

		ϵ values	Step 1 (eV)	Step 2 (eV)		Step 3 (eV)	Step 4 (eV)	Step 5 (eV)[1]	Step 6 (eV)[1]
				Step 2-1	Step 2-2				
Half PVP monolayer coverage	**Ag(100)**		0.36±0.04	152.9±2.5		31.0±1.7	-11.0±1.1	-900.6±1.1	-0.036±0.002
	Ag(111)		0.30±0.04	149.3±2.5				-828.2±1.1	-0.013±0.006
Full PVP monolayer coverage	**Ag(100)**		0.44±0.09	170.8±2.0		30.5±2.0	-11.0±1.0	-900.6±1.1	-0.036±0.002
	Ag(111)		0.44±0.07	166.5±2.9				-828.2±1.1	-0.013±0.006
LJ	**Ag(100)**	**ϵ = 0.1**	0.40±0.06	333.0±2.4	118.6±1.7	25.9±2.0	-8.19±0.8	-900.6±1.1	-0.036±0.002
		ϵ = 0.08		234.4±1.9					
		ϵ = 0.064		156.3±1.9					
		ϵ = 0.048		75.9±1.0					
		ϵ = 0.032		24.1±1.0					
		ϵ = 0.016		2.23±0.4					
	Ag(111)	**ϵ = 0.1**	0.41±0.07	361.5±2.4	123.7±1.8			-828.2±1.1	-0.013±0.006
		ϵ = 0.08		256.1±1.8					
		ϵ = 0.064		173.2±1.7					
		ϵ = 0.048		86.4±1.0					
		ϵ = 0.032		29.4±0.8					
		ϵ = 0.016		2.39±0.5					

2.2 Thermodynamics Integrand Curves

The thermodynamic integrand curves in Step 1 through 4 for PVP-EG-Ag systems are given in Figs. S1 and S2.

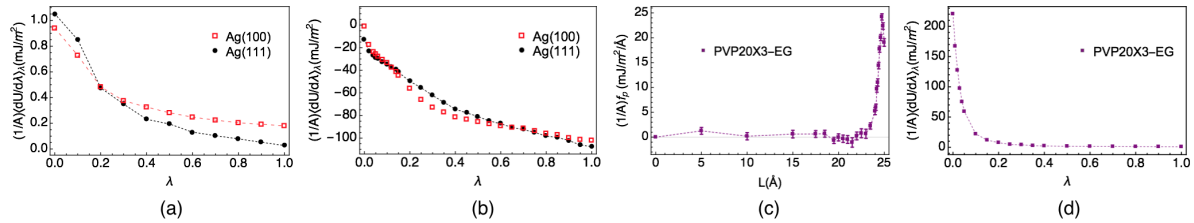

Figure S1: Thermodynamic integrands per unit area for Steps 1 to 4 in the half-coverage PVP-EG-Ag system. Error bars reflect the standard error of the mean and are omitted if smaller than the marker size. (a) Step 1; (b) Step 2; (c) Step 3; (d) Step 4.

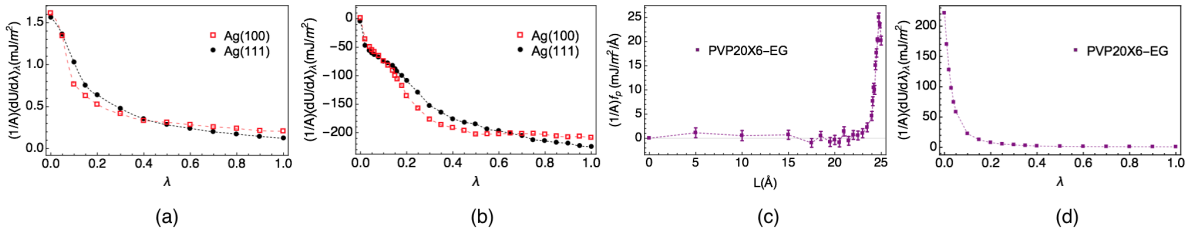

Figure S2: Thermodynamic integrands per unit area for Steps 1 to 4 in the full-coverage PVP-EG-Ag system. Error bars reflect the standard error of the mean and are omitted if smaller than the marker size. (a) Step 1; (b) Step 2; (c) Step 3; (d) Step 4.

The thermodynamic integrand curves in Steps 1, 2-2, 3 and 4 for the LJ-EG-Ag systems are given in Fig. S3. Curves for each interaction strength in Step 2-1 are summarized in Fig. S4.

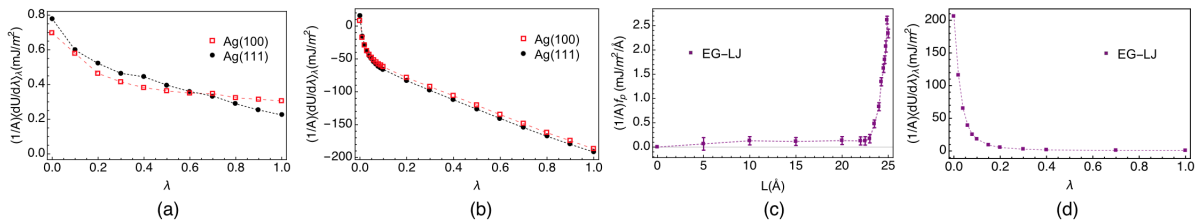

Figure S3: Thermodynamic integrands per unit area for Steps 1, 2-2, 3 and 4 in LJ-EG-Ag system. Error bars reflect the standard error of the mean and are omitted if smaller than the marker size. (a) Step 1; (b) Step 2-2; (c) Step 3; (d) Step 4.

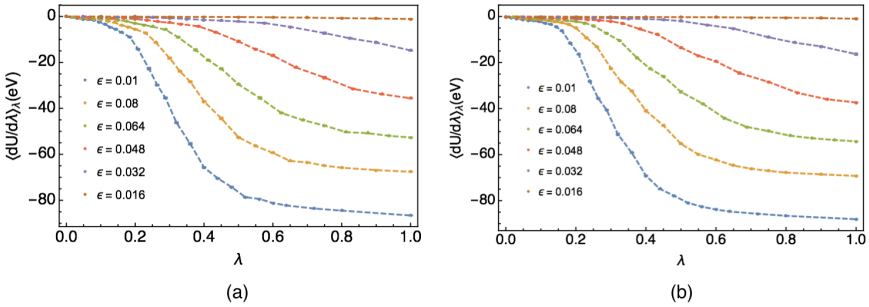

Figure S4: Thermodynamic integrands per unit area for Steps 2-1 in LJ-EG-Ag system. Error bars are omitted because they are smaller than the marker size. (a) Ag(100) systems, and (b) Ag(111) systems.

3 Hysteresis

EG, Ag and LJ particles are relatively small species, for which full relaxation can be reached within 1 ns, so most steps requires only 1∼2 ns for equilibration and sampling. This has been tested and confirmed in the Supplementary Materials of Qi et al.[7]. They also point out that Step 2 may be subject to hysteresis if sampling is not sufficient, especially for large molecules with slow relaxation. Considering the polymeric nature of PVP and its strong adsorption on Ag, the conformation adjustment at each λ when turning off PVP-Ag interactions could require more simulation time than in other steps (cf., Table S2) .

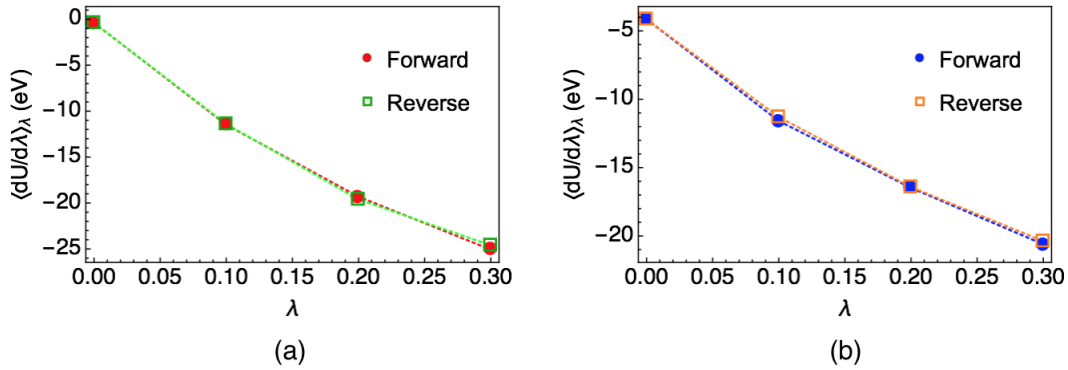

Figure S5: Forward and reverse paths for half-coverage PVP-EG-Ag systems. Error bars omitted because they are smaller than the marker size. (a) Ag(100) and (b) Ag(111).

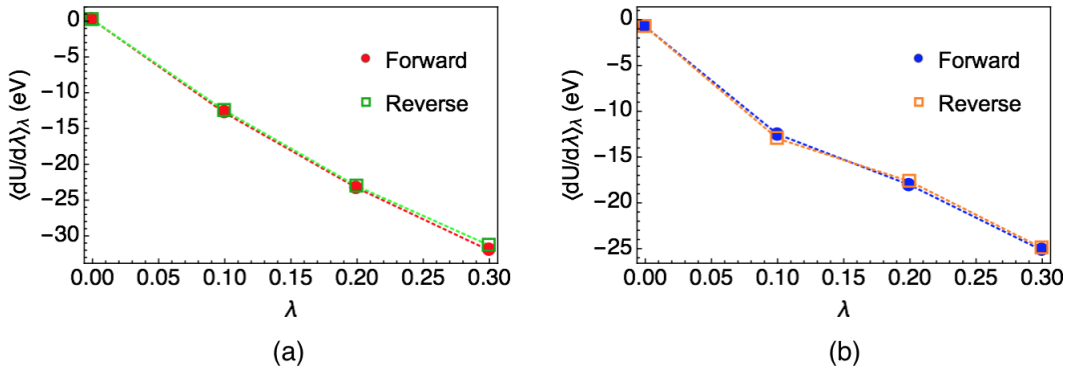

Figure S6: Forward and reverse paths for full-coverage PVP-EG-Ag systems. Error bars omitted because they are smaller than the marker size. (a) Ag(100) and (b) Ag(111).

To show that our results are hysteresis-free, we performed a reverse path simulation at critical places for both half- and full-coverage systems. During the forward pathway in Step 2,

we notice that the PVP film grows thicker without changing much of its conformation when λ decreases from 1 to 0.3. The PVP film begins to leave the Ag surface when λ reaches 0.2, and has completely vacated the surface then λ approaches 0. We consider the value of λ at which the PVP film changes its conformation from "adsorbed" to "desorbed" as the critical value at which hysteresis is the most likely to occur. Therefore, we perform a reverse run from $\lambda = 0$ to $\lambda = 0.3$, and compare the thermodynamic integrand values to the forward run. Since adsorption is usually slower than desorption, we equilibrate half- and full-coverage system for 20 and 25 ns at each λ, respectively. The forward and reverse paths are shown in Fig. S5 and S6.

References

[1] P. L. Williams, Y. Mishin and J. C. Hamilton, *Model. Simul. Mater. Sci. Eng.*, 2006, **14**, 817–833.

[2] K. Vanommeslaeghe, E. Hatcher, C. Acharya, S. Kundu, S. Zhong, J. Shim, E. Darian, O. Guvench, P. Lopes, I. Vorobyov and A. D. J. MacKerell, *J. Comput. Chem.*, 2010, **31**, 671–690.

[3] Y. Zhou, W. A. Saidi and K. A. Fichthorn, *J. Phys. Chem. C*, 2014, **118**, 3366–3374.

[4] K. A. Fichthorn, T. Balankura and X. Qi, *CrystEngComm*, 2016, **18**, 5410–5417.

[5] S. Grimme, *J. Comput. Chem.*, 2006, **27**, 1787–1799.

[6] S. Plimpton, *J. Comput. Phys.*, 1995, **117**, 1–19.

[7] X. Qi, Y. Zhou and K. A. Fichthorn, *J. Chem. Phys.*, 2016, **145**, 194108.